Chapter in SQUID Applications to Geophysics
H. Weinstock & W. Overton, eds.
Society of Exploration Geophysicists
1981

SQUIDs AND THEIR SENSITIVITY FOR GEOPHYSICAL APPLICATIONS*

Charles M. Falco** and Ivan K. Schuller**

ABSTRACT

Superconducting Quantum Interference Devices (SQUIDs) have been extensively studied over the last decade and a half. They have been developed to a point where a variety of measurements are now possible with a sensitivity that wasn't considered feasible 15 years ago. This paper reviews the physical principle behind the operation of these devices. Our intention is to enable the reader with limited familiarity with superconductivity to understand their basic operation, as well as to understand their sensitivity and potential for further development.

I. INTRODUCTION

The development of SQUIDs is a direct consequence of theoretical predictions made in 1962 (Josephson, 1962). Josephson predicted that a "supercurrent" could flow between two superconductors without a voltage drop, even though they were physically separated by a small insulating gap [see Figure (1)]. His prediction was confirmed experimentally a year later (Anderson and Rowell, 1963). It has been found that other types of structures ("weak links") also exhibit the "dc Josephson effect" as well. Some examples of Josephson "weak links" are shown in Fig. (2).

Josephson's prediction, coupled with the macroscopic quantum nature of the superconducting state, has led to the development of the highly sensitive SQUID magnetometers discussed here. This quantum nature permits us to describe the superconducting state by a single wavefunction $\psi = |\psi|e^{i\phi}$ where ϕ is the phase. In order that the wavefunction be single valued in traversing any closed loop path within the superconductor, its phase may change by at most $2\pi n$ where n is an integer. (A condition equivalent to the Bohr-Sommerfeld quantization of the hydrogen atom.) Thus the absolute value of is not important; however its spatial variation is. The difference in phase between two points within a superconductor is related to the canonical momentum by

$$\Delta\phi = 2m\vec{v}_s/\hbar + 2e\vec{A}/\hbar \qquad (1)$$

where m and e are the electronic mass and charge respectively, v_s is the velocity of the superconducting electrons, A is the vector potential, and h is Planck's constant divided by 2π. The one other concept needed to understand a superconducting magnetometer is that, according to Josephson's theory, the phase changes in crossing a weak link by an amount

$$\Delta\phi_{w\ell} = \sin^{-1}(I_s/I_c) \qquad (2)$$

where I_s is the electrical current in the weak link and I_c is the maximum possible supercurrent or "critical" current. The exact nature of the process which gives rise to the $\Delta\phi_{w\ell}$ is not understood for all weak links. However, that such a phase could change should occur is fairly clear.

If we consider two, separate bulk pieces of superconductors, the wave function in each is constant throughout, but the value in one is independent of the other. If the two are brought together, the wave functions arrange themselves to be the same since this is the state of minimum energy. In the intermediate case, where the two are very weakly connected, the phases are coupled. A supercurrent I_s can flow through such a weak link with no voltage drop, and this supercurrent causes a phase difference $\Delta\phi_{w\ell}$ to occur across it since the weakness of the coupling doesn't allow the superconductor to maintain zero phase difference. The Josephson coupling energy $\hbar i_c/2e$ has a value of 3.3×10^{-22} J for an I_c of 1 μA. This is an order of magnitude larger than the energy contained in thermal fluctuations at 4.2 K. Thus, thermal noise is not a serious consideration in most properties of SQUIDs.

The total critical current I_c that can flow before a voltage is developed is determined by the properties of the two weakly coupled superconductors and is typically 1-10 A for the weak link in a SQUID.

II. PRINCIPLES OF OPERATION

Deriving the essential properties of a SQUID is now quite straightforward (Silver and Zimmerman, 1967). If we consider the change in phase in traversing the integration path shown in Fig. (3) which starts and ends at point x, we have

*Work performed under the auspices of the U.S. Department of Energy.

**Solid State Science Division, Argonne National Laboratory, Argonne, IL 60439.

$$2\pi n = \frac{2m}{\hbar} \oint \vec{v}_s \cdot d\vec{\ell} + \frac{2e}{\hbar} \oint \vec{A} \cdot d\vec{\ell} + \Delta\phi_{wl} \qquad (3)$$

where the first two terms come from the complete line integration through the superconductor, and the third term comes from the phase change across the weak link. For devices of interest to geophysicists, we can neglect the first term, and by making use of the fact that the complete line integral of the vector potential A gives the enclosed magnetic flux ϕ_{enc}, we have that

$$2\pi n = \frac{2e}{\hbar} \phi_{enc} + \sin^{-1} (I_s/I_c) \qquad (4)$$

In the presence of an externally applied dc flux ϕ_x, the internal flux will be partially shielded by a circulating supercurrent I_s so that

$$\phi_{enc} = \phi_x + LI_s \qquad (5)$$

where L is the inductance of the loop. Combining these last two equations allows us to solve for ϕ_{enc}

$$\phi_{enc} = \phi_x - LI_c \sin \left[\frac{2\pi}{\phi_0} (\phi_{enc} - n\phi_0) \right] \qquad (6)$$

where ϕ_0 the "magnetic flux quantum" is the amount in which flux would be quantized in a bulk, hollow cylinder containing no weak link ($\phi_0 = h/2e \cong 2\times10^{-15}$ Wb). Because of the term $\Delta\phi_{wl}$, the presence of a weak link allows magnetic flux of other than a multiple of ϕ_0 to be trapped in a SQUID. Consequently, changes in the trapped flux of less than ϕ_0 can be measured. The solution to Eq. (6) for one particular value of critical current is shown in Fig. (4). This figure illustrates the essential features needed to understand the behavior of a SQUID. Starting at point A in Fig. (4), the external flux ϕ_x is increased to point B. During this time shielding currents are set up in the ring partially counteracting the external flux so that the enclosed flux increases only slightly. Beyond point B the shielding currents have exceeded the critical current of the weak link and one flux quantum ϕ_0 is admitted to the SQUID bringing it to C. At the time a flux quantum is admitted, the shielding currents decay to zero and we are left with flux trapped in the ring and no circulating current. If ϕ_x is now reduced, the upper path is followed to D due to shielding currents flowing in the opposite sense as before at which point the critical current is again exceeded and a transition returns it to the lower path. The area enclosed in the hysteresis loop ABCD is approximately ϕ_0^2, and the total energy dissipated in traversing it is ϕ_0^2/L (approximately 10^{-21} Joules). In practice, the SQUID is operated at some rf frequency ν of order 20 MHz (Zimmerman, 1972) which causes a power of order $\phi_0^2 \nu/L \cong 10^{-14}$ Watts to be dissipated. This is quite easily detected and forms the basis for the operation of these devices.

A simplified circuit diagram is shown in Fig. 5. An rf oscillator drives a "tank circuit" which is inductively coupled to the SQUID. The voltages developed in the tank circuit when the SQUID traverses a hysteresis loop are amplified and detected by room temperature electronics. The output from these electronics can be displayed in the manner of Fig. 6. As can be seen, the response is periodic as a function of external flux ϕ_x, and a small fraction of ϕ_0 can be detected. In practice, changes of less than 10^{-4} ϕ_0 can be resolved. Although the general features discussed here are valid, a precise description requires a considerably more complex circuit analysis of the entire system (Silver and Zimmerman, 1967). Commercially available instruments make use of some variation of the basic "rf SQUID" described above. Some examples of rf SQUIDs are shown in Fig. 7.

There is a second type of device, the "dc SQUID," which isn't as widely used as the rf SQUID even though its sensitivity is at least as good. Since the same general quantum mechanical principles are used in describing the behavior of this device, which is made up of two weak links in a loop of superconductor, we will refer the reader interested in a complete description to the article by Clarke (Clarke, 1973). Examples of dc SQUIDs are shown in Fig. 8.

III. SENSITIVITY

All SQUIDs must be made from superconducting materials; consequently they require dewars, cryogenic liquids or refrigeration devices to maintain low enough temperatures (near or below 15 K). What advantages do SQUIDs have over conventional devices? The answer is both sensitivity and frequency response. Various measures of sensitivity can be used which depend on the intended application. However, the intrinsic sensitivity of a SQUID is best measured in terms of its energy resolution; that is, the minimum energy which, when applied to the input of the device, produces a measurable response. Present commercial SQUIDs have an energy resolution of approximately 10^{-30} Joules when measured with a 1 Hz output bandwidth. To give some idea of how sensitive these devices are, we note that this energy resolution corresponds to the kinetic energy that a single hydrogen atom would gain falling a distance of only 0.1 mm in the earth's gravitational field.

The most sensitive SQUIDs produced to date have been made at the IBM Thomas J. Watson Research Laboratory (Voss, Laibowitz, Ketchen, and Broers, 1980). They have reported sensitivities greater than 2×10^{-33} J/Hz. This is within a factor of 3 of Planks constant h and therefore within a factor of 6 of the ultimate limit of approximately h/2 (Tesche and Clarke, 1977). However, this final increase of sensitivity, while welcome, is unlikely to have major impact on geophysical measurements.

As discussed by S. Breiner in an accompanying article, conventional induction coil magnetometers can compete favorably with SQUIDs in the frequency range above 1 Hz. However, as shown in Fig. 10, measurements made at these "high" frequencies can be sensitive to relatively shallow depths, depending on the conductivity of the earth at a particular location. It is at "low frequencies, below 1 Hz, where the extremely low 1/f noise of a SQUID offers its greatest advantage while the SQUID and induction

coil magnetometer may have roughly identical sensitivities at 1 Hz, the SQUID is four orders of magnitude better at .01 Hz. There is a clear advantage in MT applications where it is necessary to invert low frequency data to high precision.

Due to the zero electrical resistance of a superconducting coil, it is possible to induce a non-decaying current by application of a static magnetic field. As depicted in Fig. 11, this makes it possible to wind a flux transformer which induces a static magnetic field in the secondary due to the application of a dc field to the primary (Giffard, Webb, and Wheatley, 1972). If the primary is carefully wound as two identical, separate coils in opposition, the secondary will only carry a current (and hence produce a magnetic field) if a magnetic field gradient exists near the primary. Any effects due to dc fields, such as from the earth, are reduced very effectively using these first derivative gradiometers. The present limit on gradient sensitivity is roughly 2×10^{-4} γ/m with a spatial resolution of 20 cm (Gillespie, Podney, and Buxton, 1977). In the case of gradiometric data, the SQUID is unrivaled at all frequencies. A SQUID gradiometer offers its high gradient sensitivity with a spatial resolution of much less than 1 meter. Also, unlike operating two magnetometers in opposition, the SQUID gradiometer coils are rigidly coupled so that balancing, motional stability, and vibrational problems are eliminated. Where gradiometric data is required, as in location of lateral spatial inhomogeneities, the extremely high sensitivity of a SQUID coupled with its spatial resolution of less than 20 cm, makes it highly advantageous.

It should be pointed out that higher order derivatives with comparable sensitivites can also be easily obtained using SQUIDs and properly wound flux transformers.

Other SQUID systems of interest to geophysicists include rock magnetometers (Goree and Fuller, 1976) and susceptometers (Philo and Fairbank, 1977). The rock magnetometers have magnetic moment sensitivities of 10^{-8} emu along 3 axes over sample volumes as large as 10 cm diameter. Susceptometers offer the same level of moment sensitivity, susceptibility sensitivity of 10^{-11} emu/cm^3 at 1 kG, and frequency response up to a few kHz. In both cases, improvements of several orders of magnitude can be expected in the future.

IV. SUMMARY AND CONCLUSION

We have described the physical principles underlying the operation of SQUIDs. The sensitivity of current commercial devices as well as projected future increases in sensitivity have also been discussed to enable comparison with competing, conventional devices.

ACKNOWLEDGMENTS

We are pleased to acknowledge conversations with M. Gershenson and financial support by the Solid State Physics and Materials Chemistry Branch of the U.S. Department of Energy.

REFERENCES

Anderson, P. W. and Rowell, J. M., 1963, Possible Observation of the Josephson Superconducting Tunneling Effect, Phys. Rev. Letters, Vol. 10, p. 230-234.

Clarke, J., 1973, Low Frequency Applications of Superconducting Quantum Interference Devices, Proc. IEEE, Vol. 61, p. 8-19.

Giffard, R. P., Webb, R. A., and Wheatley, J. C., 1972, Principles and Methods of Low Frequency Electric and Magnetic Measurements Using an rf-Biased Point-Contact Superconducting Device, J. Low Temp. Phys., Vol. 6, p. 533-610.

Gillespie, G. H., Podney, W. N., and Buxton, J. L., 1972, Low-Frequency Noise Spectra of a Superconductivity Magnetic Gradiometer, J. Appl. Phys., Vol. 48, p. 354-357.

Goree, W. S. and Fuller, M., 1976, Magnetometer Using RF-Driven SQUIDs and Their Applications in Rock Magnetism and Paleomagnetism, Rev. Geophysics and Space Phys., Vol. 14, p. 591-598.

Josephson, B. D., 1962, Possible New Effect in Superconductive Tunneling, Phys. Letters, Vol. 1, p. 251-253.

Philo, J. S. and Fairbank, W. M., 1977, High-Sensitivity Magnetic Susceptometer Employing Superconducting Technology, Rev. Sci. Instrs., Vol. 48, p. 1529-1536.

Silver, A. H. and Zimmerman, J. E., 1967, Quantum States and Transitions in Weakly Connected Superconducting Rings, Phys. Rev., Vol. 157, p. 317-341.

Tesche, C. D., and Clarke, J., 1977, dc SQUID: Noise and Optimization, J. Low Temp. Phys., Vol. 29, p. 301-331.

Voss, R. F., Laibowitz, R. B., Ketchen, M. B., and Broers, A. N., 1980, Proceedings of Second International Coinference on SQUIDs, Berlin, to be published.

Zimmerman, J. E., 1972, Josephson Effect Devices and Low-Frequency Field Sensing, Cryogenics, Vol. 12, p. 19-31.

FIGURES

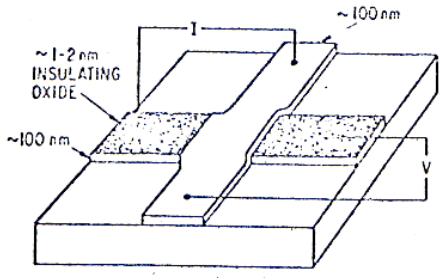

Fig. 1. Superconductor-Insulator-Superconductor Josephson tunnel junction.

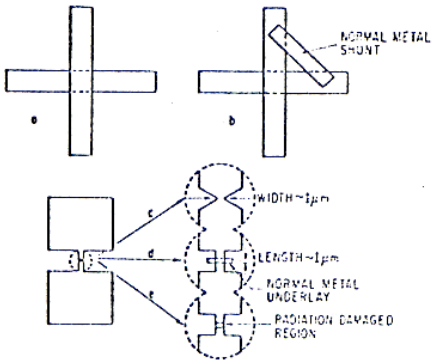

Fig. 2. Several types of Josephson weak links: (a) tunnel junction, (b) shunted tunnel junction, (c) Dayem bridge, (d) proximity effect, (e) radiation damaged.

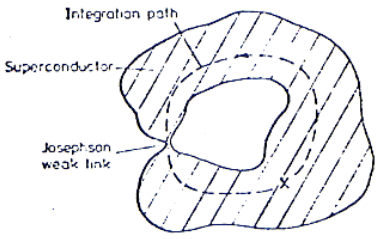

Fig. 3. Conceptual diagram of a SQUID.

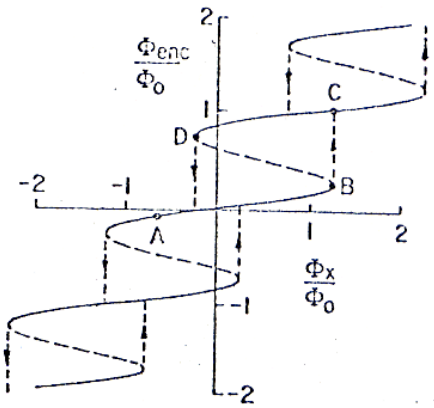

Fig. 4. SQUID response to an external dc magnetic flux.

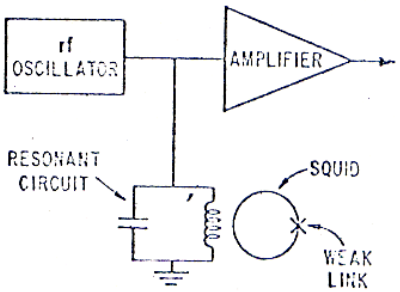

Fig. 5. Block diagram of electronics used to operate a SQUID.

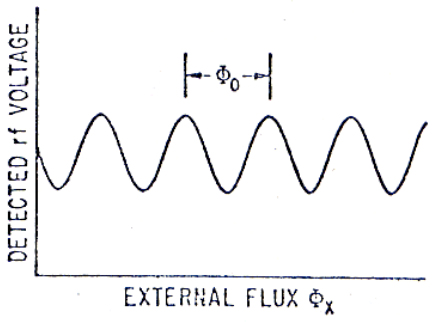

Fig. 6. Output from SQUID electronics as a function of applied magnetic flux.

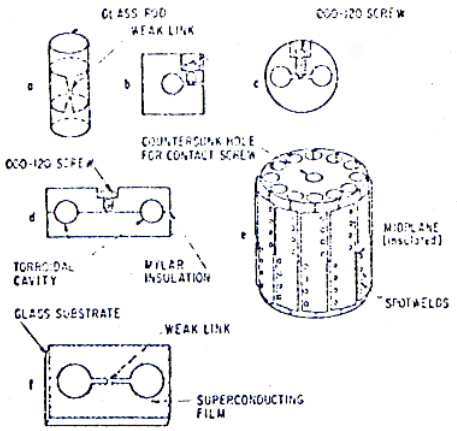

Fig. 7. Several types of rf SQUIDs: (a) cylindrical thin film, (b) bulk point contact, (c) point contact gradiometer, (d) toroidal point contact, (e) low inductance, multihole, (f) planar thin film.

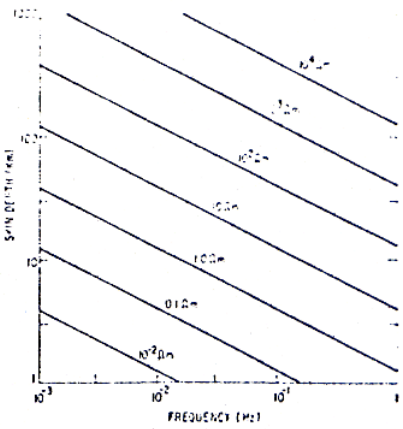

Fig. 9. Skin depth of the earth as a function of frequency for various resistivities.

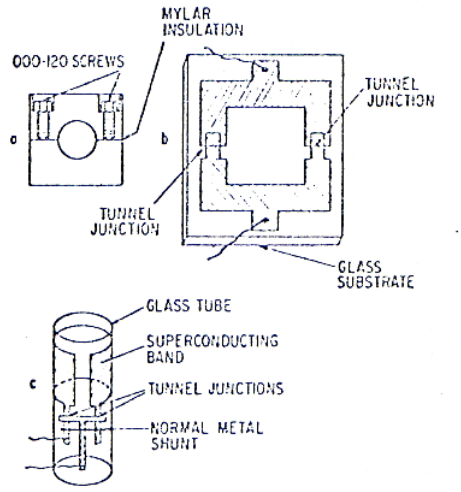

Fig. 8. Several types of dc SQUIDs: (a) bulk point contact, (b) planar thin film, (c) cylindrical thin film.

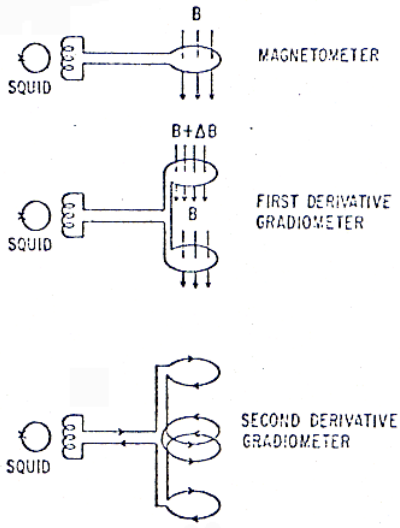

Fig. 10. Various flux transformer configurations.